ISSN (Print) 1226-1750
ISSN (Online) 2233-6656
**Journal of Magnetics** 30(4), 705-711 (2025) https://doi.org/10.4283/JMAG.2025.30.4.705

# Track Misregistration Prediction Scheme of Two-Track Reading with a Wide-Track Reader for Shingled Track Recording

**P. Kochcha, A. Khametong, K. Kankhunthod*, and C. Warisarn**

*School of Integrated Innovative Technology (SIITec), King Mongkut's Institute of Technology Ladkrabang (KMITL), 1 Chalonkrung rd., Ladkrabang Bangkok 10520, Thailand*

(Received 19 May 2025, Received in final form 12 December 2025, Accepted 15 December 2025)

**To enhance the areal density (AD) of magnetic recording technology, shingled magnetic recording (SMR), which overlaps adjacent tracks, has been proposed and extensively studied. The strong intertrack interference (ITI) is a major difficulty that needs to be overcome. Therefore, the two-track reading with a wide-track reader for the shingled track recording technique achieves the clear amplitude in two-track recording due to the longer bit length of magnetization over the regular single-track reading. Track misregistration (TMR); however, is one of the key concerns in this technique that may deteriorate the system's performance, which refers to the misalignment between the center of the read head and the desired track. To address this issue, this study proposes the TMR prediction scheme and detector with the utilization of an Expectation-Maximization (EM) algorithm to process the readback signals obtained from the wide-track reader. Simulation results indicate that, at an AD of 2.0 Tb/in$^2$, the EM-based TMR prediction method achieves strong prediction performance, while the EM-based data detector further enhances system performance by reducing the bit-error rate in shingled track recording systems.**

**Keywords :** wide-track reader, shingled track recording, track misregistration (TMR), expectation-maximization (EM) algorithm

## 1. Introduction

Shingled magnetic recording (SMR) is an advanced data storage technology designed to increase areal density (AD) of hard disk drives (HDDs) [1]. It writes data tracks by partially overlapping them, similar to the way shingles are layered on a roof. This overlapping enables the formation of narrower tracks, allowing more data to be stored on the same platter surface and thereby enhancing AD. However, the reduced track width increases inter-track interference (ITI) and makes the system more susceptible to track misregistration (TMR)—a condition where the read-head deviates from the center of the narrow track during data retrieval. This misalignment significantly degrades the read performance of magnetic recording systems [2-4].

In conventional HDDs, TMR is typically monitored through a servo mechanism [5] that reads dedicated servo data embedded on the disk surface. While effective, this approach consumes valuable disk space—typically 3% to 5% [6]—that could otherwise be used for user data. To address this limitation, recent research has focused on TMR prediction methods that operate without servo data, aiming to recover accurate positional information directly from the readback signal [6-8].

Recent advances in magnetic recording have increasingly focused on data-driven and machine-learning-assisted strategies to improve TMR estimation under severe interference conditions. Multi-reader signal analysis has been used to reconstruct the position error signal (PES) via adaptive equalizer coefficients in SMR systems [6]. Adaptive 2D equalization has also been proposed, where TMR levels are estimated from the ratio of 2D equalizer coefficients and mitigated using asymmetric equalization targets [7]. In addition, clustering-based approaches such as K-means have demonstrated promising results by estimating TMR from the centroid of readback signals, followed by TMR-aware equalization and detection [8]. These methods have contributed to notable progress. However, these mentioned techniques [7, 8] were proposed


*Corresponding author: Tel: +669-4949-5392
e-mail: kittipon.ka@kmitl.ac.th

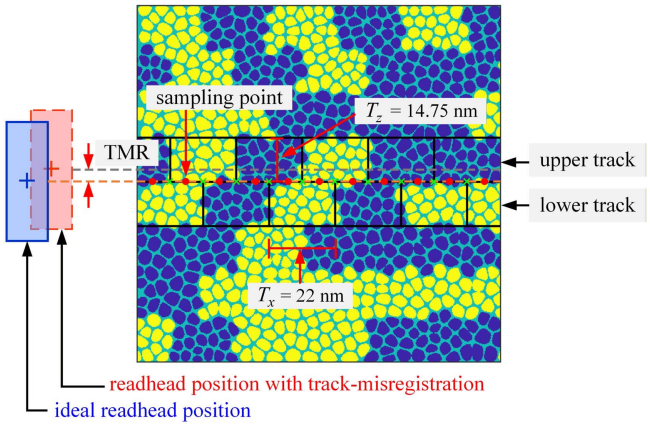


**Fig. 1.** (Color online) Recorded magnetization allocation in granular media using the two-track reading with a wide-track reader.

for bit-patterned media recording.

In this study, therefore, we propose a TMR prediction and mitigation framework based on the Expectation-Maximization (EM) algorithm for granular media. The system configuration adopts staggered alignment of adjacent tracks [9], as shown in Fig. 1. First, an EM-based TMR predictor estimates the TMR level directly from the readback signal. The estimated TMR level is then used to select suitable one-dimensional (1D) equalizer coefficients. Subsequently, an EM-based data detector performs probabilistic clustering for bit detection. By jointly applying the EM algorithm in both the prediction and detection stages, the proposed method effectively models variations in the readback signal and enhances robustness against TMR-induced distortions. This unified two-stage EM-based approach results in improved bit-error rate (BER) performance in staggered SMR systems.

The remainder of this paper is structured as follows: Section 2 introduces the staggered SMR recording model. Section 3 presents the proposed EM-based TMR predictor and data detector. Section 4 discusses the simulation results, and Section 5 concludes the paper.

## 2. Channel Model

The staggered SMR system model is illustrated in Fig. 2, which presents a block diagram outlining the data flow from the recording process to data retrieval.

In the pre-coding process, the input user bit sequence $\{a_k\}$, consists of 8,160 bits, each with value $a_k \in \{+1, -1\}$, where $k$ denotes the bit index. This sequence is first passed through a pre-coding stage, defined in Table 1 [9], to generate the pre-coded sequence $\{c_k\}$. The pre-coding process is a state-dependent mapping that utilizes the current input bit $a_k$ and the previous output bit $c_{k-1}$. For instance, when $a_k = +1$, the resulting output $c_k$ is determined based on the value of $c_{k-1}$: if $c_{k-1} = -1$, then $c_k$ is set to -1; conversely, if $c_{k-1} = +1$, then $c_k = +1$ [9].

In the recording sequences, the pre-coded sequence $\{c_k\}$ is divided into two subsequences that are the even-indexed sequence $\{c_{k,0}\}$ and the odd-indexed sequence $\{c_{k,1}\}$. These subsequences are recorded on the lower and upper tracks, respectively.

With respect to the recording medium, this study considers the SMR system illustrated in Fig. 1. The separated pre-coded sequences $\{c_{k,0}\}$ and $\{c_{k,1}\}$ are written to a pair of considered tracks in a staggered pattern. The two tracks are offset by half a bit length, allowing for higher track density. This study focuses on an SMR configuration with an AD of 2.0 terabits per square inch (Tb/in$^2$), where the track-width $\{T_z\}$ and the bit-length $\{T_x\}$ are set to 14.75 nanometers (nm) and 22.0 nm, respectively.

In the reading process, to retrieve the continuous readback signal $\{r(t)\}$, the wide-track reader is positioned at the midpoint between the upper and lower tracks, as illustrated in Fig. 1. This placement enables simultaneous reading of both tracks. The resulting signal is generated through a 2D convolution of the reader's sensitivity function [10] with the magnetization pattern of the granular media, also shown in Fig. 1. To suppress out-of-

**Table 1.** Pre-coding logic for input-to-output bit mapping.

| $k^{\text{th}}$ Input bit $a_k$ | $k$-1$^{\text{th}}$ output bit ($c_{k-1}$) | $k^{\text{th}}$ Output bit ($c_k$) |
|---|---|---|
| +1 | -1 | -1 |
| +1 | +1 | +1 |
| -1 | +1 | -1 |
| -1 | -1 | +1 |

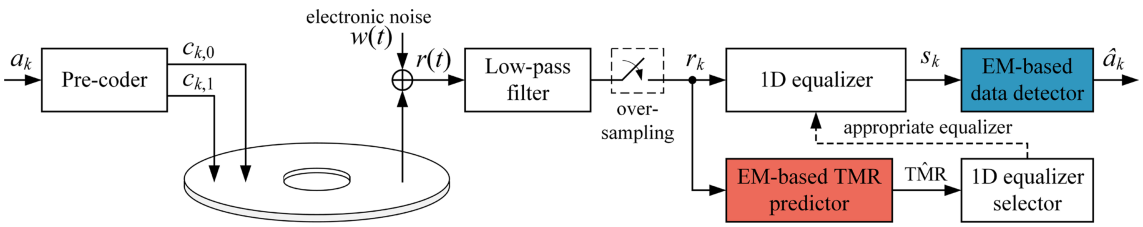


**Fig. 2.** (Color online) Channel model of the SMR systems with the proposed EM-based TMR predictor and detector.

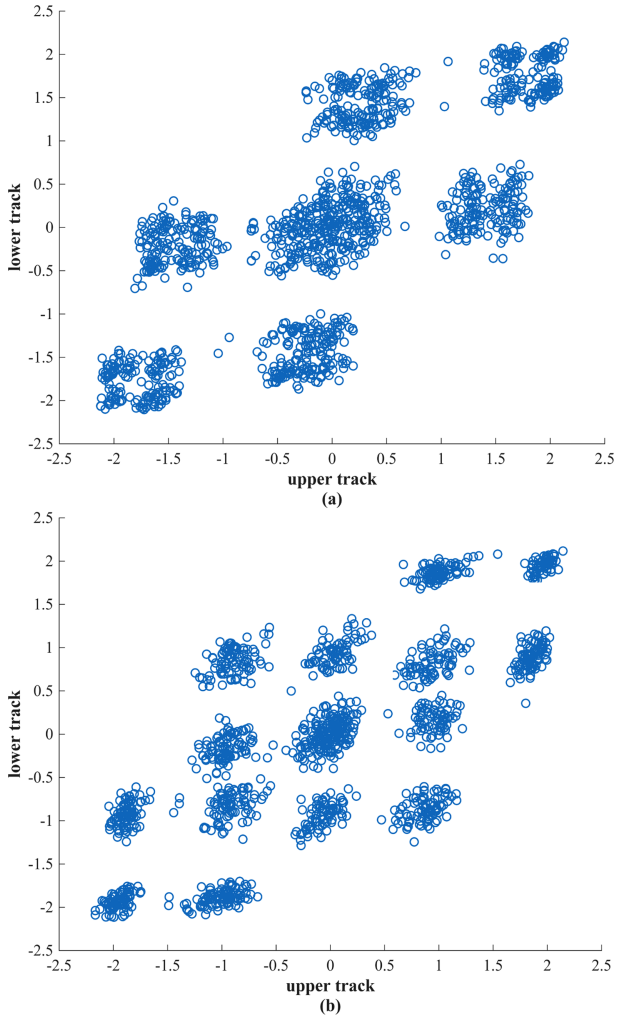


**Fig. 3.** (Color online) The scatting plot of the readback signal, for (a) $0.25T_x$ and (b) $0.50T_x$ sampling scheme.

band noise, the readback signal is filtered using a seventh-order Butterworth low-pass filter (LPF) with a cutoff frequency of $0.50/T_x$. The filtered signal is then over-sampled at a rate of $0.50T_x$, starting at one-fourth of the bit period ($0.25T_x$) as indicated by the red dots in Fig. 1, to produce the discrete-time readback signal $\{r_k\}$. This sampling scheme differs from that of the transition-based sampling (green crosses in Fig. 1, starting at $0.50T_x$), as illustrated in Fig. 3.

Fig. 3(a) and 3(b) present the scatter plots of the readback signals obtained from the $0.25T_x$ and $0.50T_x$ sampling schemes, respectively. The $x$- and $y$-axis represent the amplitudes of the even and odd readback sequences at a TMR level of 0 nm without electronic noise. The $0.25T_x$ scheme exhibits fewer and more compact clusters, whereas the $0.50T_x$ scheme produces more dispersed clusters under noise. Therefore, the $0.25T_x$ sampling scheme is adopted in this study due to its clearer clustering characteristics, which are more suitable for clustering-based TMR estimation.

The TMR mitigation process consists of two main components: TMR level prediction and data detection, both based on the EM algorithm, which is discussed further in Section 3. The discrete readback signal $\{r_k\}$ is first fed to the EM-based TMR predictor, which predicts the TMR level in the system. Based on this predicted level, appropriate 1D equalizer coefficients are selected to equalize the readback signal, producing the equalized sequence $\{s_k\}$. This sequence is then processed by the proposed EM-based data detector, which simultaneously retrieves the output bit sequence $\{\hat{a}_k\}$ and compensates for the effects of TMR, thereby improving the overall BER performance.

## 3. Proposed Methods

The proposed method consists of two main components, described as follows:

### 3.1. EM-based TMR predictor

The TMR level is estimated using the EM algorithm—an iterative procedure commonly used to compute the maximum likelihood estimates of parameters (e.g., means and variances) in statistical models involving latent (unobserved) variables [11].

Predetermined centroid method: The discrete readback signal $\{r_k\}$, consisting of 8,160 samples obtained from the SMR system under various TMR levels (i.e., TMR $\in$ {-3.0, -2.5, …, 0, …, 2.5, 3.0} nm), is reshaped into a 2×4,080 matrix by separating the samples into odd- and even-indexed values. Each column of this matrix forms a 2D data point, which serves as input for clustering using the EM algorithm, resulting in predetermined centroids $\{\hat{\mathbf{C}}_{\text{TMR}}\}$ illustrated in Table 2.

The EM algorithm operates iteratively through two primary steps: the expectation step (E-step) and the maximization step (M-step). The E-step calculates the probability that each 2D data point belongs to one of the initial clusters (centroids). In this case, seven clusters are defined as {[-2, -2], [-2, 0], [0, -2], [0, 0], [0, +2], [+2, 0], [+2, +2]} corresponding to the seven possible TMR levels. The probability distribution in the E-step is modeled using the normal probability density function (PDF), expressed as follows:

$$f(x\,|\,\mu,\sigma)=\frac{1}{\sqrt{2\pi\sigma^2}}\exp\left[\frac{-(x-\mu)^2}{2\sigma^2}\right],\ \text{for}\ x\in\mathbb{R}, \tag{1}$$

where $x$ represents a column vector from the readback

**Table 2.** The centroid list for TMR, based on the EM algorithm, ranges from -3.0 nm to 3.0 nm.

| Centroid list from EM algorithm | | | | | | | | | | | | | | |
|---|---|---|---|---|---|---|---|---|---|---|---|---|---|---|
| $\hat{\mathbf{C}}_{\mathrm{TMR=0.0\,nm}}$ | | $\hat{\mathbf{C}}_{\mathrm{TMR=0.5\,nm}}$ | | $\hat{\mathbf{C}}_{\mathrm{TMR=1.0\,nm}}$ | | $\hat{\mathbf{C}}_{\mathrm{TMR=1.5\,nm}}$ | | $\hat{\mathbf{C}}_{\mathrm{TMR=2.0\,nm}}$ | | $\hat{\mathbf{C}}_{\mathrm{TMR=2.5\,nm}}$ | | $\hat{\mathbf{C}}_{\mathrm{TMR=3.0\,nm}}$ | |
| -1.79 | -1.79 | -1.78 | -1.78 | -1.77 | -1.77 | -1.76 | -1.75 | -1.74 | -1.74 | -1.72 | -1.72 | -1.70 | -1.70 |
| -1.43 | -0.20 | -1.43 | -0.26 | -1.43 | -0.31 | -1.43 | -0.36 | -1.43 | -0.42 | -1.42 | -0.47 | -1.41 | -0.52 |
| -0.25 | -1.45 | -0.30 | -1.45 | -0.35 | -1.45 | -0.40 | -1.45 | -0.45 | -1.45 | -0.50 | -1.44 | -0.55 | -1.43 |
| +0.00 | +0.00 | +0.00 | +0.00 | +0.00 | +0.00 | +0.00 | +0.00 | +0.00 | +0.00 | +0.00 | +0.00 | +0.00 | +0.00 |
| +0.24 | +1.44 | +0.29 | +1.45 | +0.35 | +1.45 | +0.40 | +1.45 | +0.45 | +1.45 | +0.50 | +1.44 | +0.55 | +1.43 |
| +1.43 | +0.20 | +1.43 | +0.26 | +1.43 | +0.31 | +1.43 | +0.36 | +1.43 | +0.41 | +1.42 | +0.46 | +1.41 | +0.52 |
| +1.79 | +1.79 | +1.78 | +1.78 | +1.77 | +1.77 | +1.76 | +1.75 | +1.74 | +1.74 | +1.72 | +1.72 | +1.70 | +1.70 |
| $\hat{\mathbf{C}}_{\mathrm{TMR=0.0\,nm}}$ | | $\hat{\mathbf{C}}_{\mathrm{TMR=-0.5\,nm}}$ | | $\hat{\mathbf{C}}_{\mathrm{TMR=-1.0\,nm}}$ | | $\hat{\mathbf{C}}_{\mathrm{TMR=-1.5\,nm}}$ | | $\hat{\mathbf{C}}_{\mathrm{TMR=-2.0\,nm}}$ | | $\hat{\mathbf{C}}_{\mathrm{TMR=-2.5\,nm}}$ | | $\hat{\mathbf{C}}_{\mathrm{TMR=-3.0\,nm}}$ | |
| -1.79 | -1.79 | -1.80 | -1.80 | -1.80 | -1.80 | -1.81 | -1.80 | -1.81 | -1.80 | -1.81 | -1.80 | -1.80 | -1.80 |
| -1.43 | -0.20 | -1.42 | -0.15 | -1.42 | -0.10 | -1.42 | -0.05 | -1.41 | -0.00 | -1.41 | +0.05 | -1.40 | +0.10 |
| -0.25 | -1.45 | -0.20 | -1.44 | -0.15 | -1.44 | -0.10 | -1.44 | -0.04 | -1.44 | +0.00 | -1.43 | +0.05 | -1.42 |
| +0.00 | +0.00 | +0.00 | +0.01 | +0.00 | +0.00 | +0.00 | +0.00 | +0.01 | +0.00 | +0.00 | +0.00 | +0.01 | +0.00 |
| +0.24 | +1.44 | +0.19 | +1.44 | +0.14 | +1.44 | +0.09 | +1.43 | +0.04 | +1.43 | -0.01 | +1.43 | -0.06 | +1.42 |
| +1.43 | +0.20 | +1.42 | +0.15 | +1.42 | +0.10 | +1.42 | +0.05 | +1.41 | -0.01 | +1.41 | -0.05 | +1.40 | -0.10 |
| +1.79 | +1.79 | +1.80 | +1.80 | +1.80 | +1.80 | +1.80 | +1.80 | +1.80 | +1.80 | +1.80 | +1.80 | +1.80 | +1.79 |

signal matrix, corresponding to a 2D data point. The initial mean (centroid) of $x$ is denoted by $\mu$, and the initial standard deviation is set to $\sigma = 1$.

In the M-step, the expected log-likelihood calculated during the E-step is maximized to update the cluster centroids, thereby improving clustering accuracy. This process is repeated iteratively until convergence is achieved. Fig. 4(a) presents an example of the 2D scatter plot of the readback signal clustered using the EM algorithm, along with the initial centroids, under a TMR condition of 2.0 nm.

TMR prediction method: the readback signal with unknown TMR is clustered by the proposed EM-based TMR predictor, producing the predicted centroids denoted by $\{\mathbf{C}_{\mathrm{TMR}}\}$ matrix as follows:

$$\mathbf{C}_{\mathrm{TMR}} = \begin{bmatrix} c_{1,1} & c_{1,2} \\ c_{2,1} & c_{2,2} \\ \vdots & \vdots \\ c_{7,1} & c_{7,2} \end{bmatrix}. \tag{2}$$

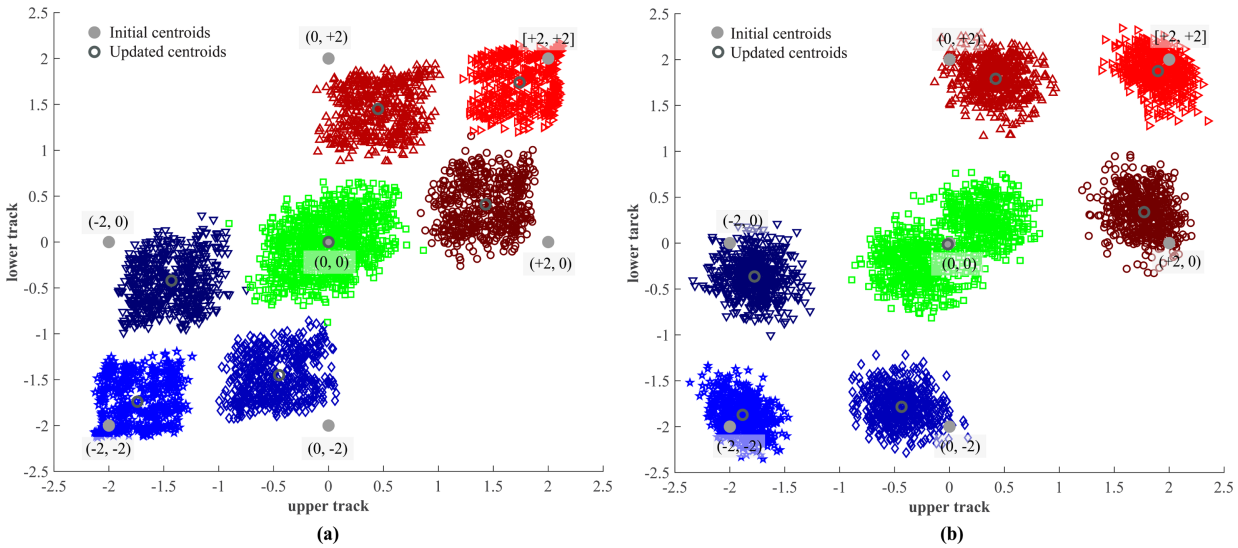


**Fig. 4.** (Color online) 2D scatter plots clustered using the EM algorithm: (a) discrete readback signal and (b) equalized readback signal.

The predicted TMR level {T$\hat{\text{M}}$R} is determined by comparing the Euclidean distance $\{d_{\text{TMR}}\}$ between the predicted centroids of the readback signal $\{\mathbf{C}_{\text{TMR}}\}$ and the sets of predetermined centroids $\{\hat{\mathbf{C}}_{\text{TMR = -3.0 nm}}, \ldots, \hat{\mathbf{C}}_{\text{TMR = 3.0 nm}}\}$; the T$\hat{\text{M}}$R is selected by $\hat{\mathbf{C}}_{\text{TMR}}$, which provides the minimum distance according to the following equation:

$$d_{\text{TMR}} = \text{Euclidean Distance}(\mathbf{C}_{\text{TMR}}, \hat{\mathbf{C}}_{\text{TMR}}) = \sqrt{\sum_{p=1}^{7}\sum_{q=1}^{2}\left(c_{p,q} - \hat{c}_{p,q}\right)^2}, \quad (3)$$

where $q$ and $p$ are the column and row indices of the matrix, respectively. After predicting the TMR level, the corresponding 1D equalizer coefficients are selected based on the estimated value to enhance data clustering before detection. Fig. 4(a) and 4(b) compare the scatter plots of the discrete and equalized readback signals, respectively. After equalization, the data clusters become more compact and clearly separated. This improvement facilitates data clustering in the EM-based detector and contributes to the overall enhancement in BER performance.

### 3.2. EM-based data detector

During the data detection stage, the equalized readback signal $\{s_k\}$ is processed by the proposed EM-based data detector, which employs the EM algorithm for clustering. The process is initialized using initial centroid values as described in Section 3.1, resulting in seven clusters.

To reconstruct the output bit sequence $\{\hat{a}_k\}$, each data point is assigned to its nearest updated centroid. The final output bit values are then determined based on the centroid-to-bits mapping specified in Table 3, which outlines the initial centroids and their associated output bits representations used throughout the detection process.

## 4. Simulation Results

### 4.1. TMR prediction accuracy

Fig. 5 illustrates the TMR prediction accuracy of the proposed EM-based TMR prediction versus the various electronic noise levels. The following equation calculates the prediction accuracy:

$$\text{Accuracy}(\%) = 100 - \frac{\left|\text{T}\hat{\text{M}}\text{R} - \text{TMR}\right|}{\text{TMR}} \times 100, \quad (4)$$

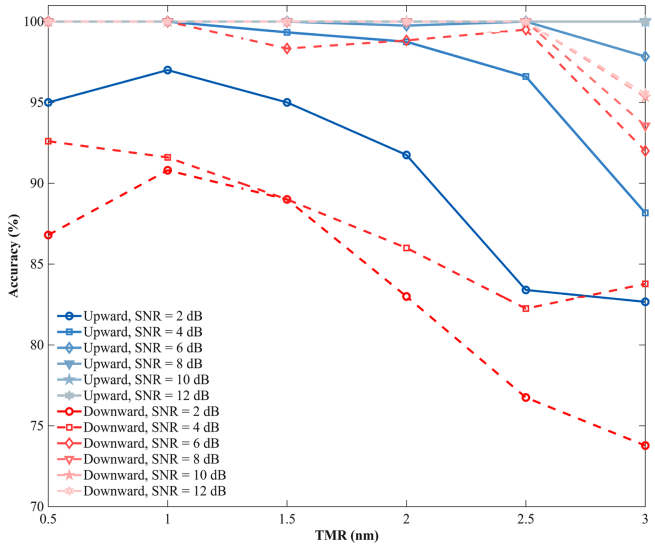


**Fig. 5.** (Color online) TMR prediction accuracy at various SNR levels under an AD of 2.0 Tb/in$^2$.

where TMR denotes the actual track misregistration level in the system, and the electronic noise levels in terms of signal-to-noise ratio (SNR), which is modeled as follows:

$$\text{SNR} = 20\log_{10}\left(A/\sigma\right), \quad (5)$$

where $A$ = 1 donates the power of the readback signal, and $\sigma$ is the standard deviation of the additive white Gaussian noise (AWGN). The shaded blue and shaded broken red lines illustrate the TMR prediction accuracy at both upward and downward TMR directions, respectively, i.e., TMR $\in$ {-3.0, -2.5, …, 0, …, 2.5, 3.0} nm across various SNR levels of {2, 4, 6, …, and 12} decibels (dBs). The EM algorithm achieves an overall prediction accuracy exceeding 70%, demonstrating strong robustness in distinguishing TMR effects. The downward TMR direction exhibits a similar trend to the upward case but yields slightly lower accuracy across all TMR and SNR conditions. This difference arises from the non-uniform magnetic grain structure of the granular media, which introduces asymmetry in the readback signal characteristics between directions. Although the prediction accuracy decreases gradually as the TMR magnitude increases and the SNR decreases, the proposed method consistently maintains accuracy above 70% even at an SNR of 2 dB,

**Table 3.** The initial centroid-to-bits mapping is used in the data detection process.

| | Centroid-to-bits output mapping | | | | | | |
|---|---|---|---|---|---|---|---|
| Initial centroids | [-2, -2] | [-2, 0] | [0, -2] | [0, 0] | [0, +2] | [+2, 0] | [+2, +2] |
| Output bits | $[+1, +1]^T$ | $[+1, -1]^T$ | $[-1, +1]^T$ | $[-1, -1]^T$ | $[-1, +1]^T$ | $[+1, -1]^T$ | $[+1, +1]^T$ |

underscoring its potential for practical implementation.

### 4.2. TMR mitigation performance

This section evaluates the TMR mitigation performance of the proposed EM-based data detector under an AD of 2.0 Tb/in$^2$. Three systems are considered: "Proposed system": A staggered SMR system employing both the EM-based TMR predictor and EM-based data detector. "System I": A baseline staggered SMR system without any TMR mitigation. The equalizer coefficients are designed based on a TMR level of 0 nm, and a simple threshold detector is used for data detection. "System II": a staggered SMR system where the TMR prediction is assumed to be 100% accurate, the equalizer coefficients are designed to match the actual TMR level, and a simple threshold detector is used for data detection.

In this study, a simple threshold detector is employed for both "System I" and "System II." Although PRML detection is generally effective for partial-response (PR) class signals, the readback waveform under the $0.25T_x$ sampling scheme does not exhibit a PR2-like characteristic, which typically presents five sample levels {−2, −1, 0, +1, +2}. Instead, it exhibits a three-level behavior {−2, 0, +2}. Consequently, PRML detection offers no performance advantage in this configuration. In contrast, the threshold detector aligns better with the signal characteristics of the $0.25T_x$ sampling scheme and achieves superior BER, particularly under high TMR conditions.

Fig. 6 presents the BER performance comparison between the upward and downward TMR directions of the proposed system. Due to the non-uniformity of magnetic grains in the recording medium, the two directions do not yield identical BER results, although they exhibit the same overall trend. Therefore, the BER comparison among the "Proposed system," "System I," and "System II" is reported only for the upward TMR direction.

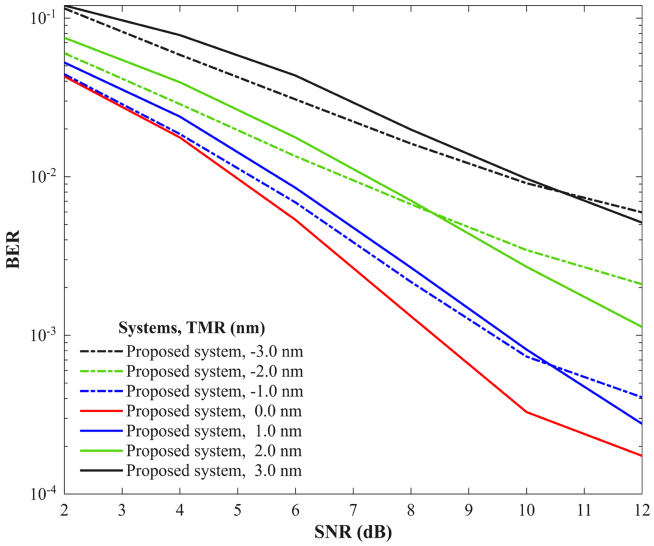


**Fig. 6.** (Color online) BER performance comparison of the "Proposed system" for upward and downward TMR directions under various TMR and SNR levels.

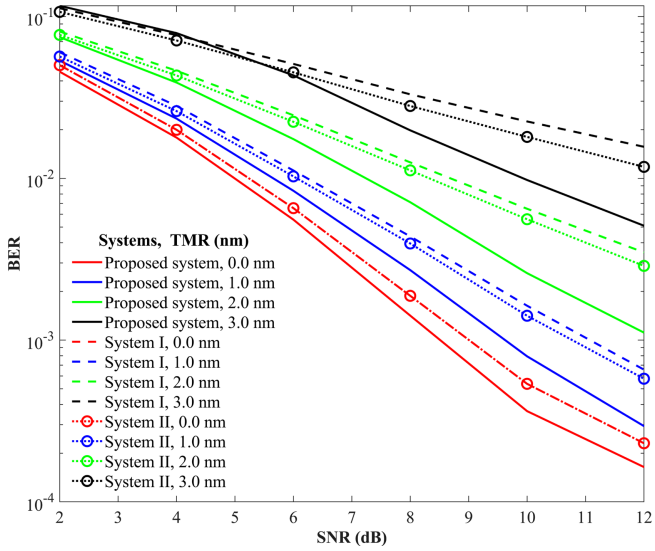


**Fig. 7.** (Color online) BER performance comparison between the Proposed system, System I, and System II at various TMR and SNR levels under the AD of 2.0 Tb/in$^2$.

Fig. 7 presents a BER performance comparison among these three systems. The results demonstrate that the "Proposed system" consistently outperforms the other two, particularly at higher SNR levels where the performance gain becomes more pronounced.

The threshold detectors in "System I" and "System II" operate in a 1D domain, making bit-by-bit decisions based on amplitude comparison with a fixed threshold. While simple, this approach cannot effectively capture inter-track interference or noise correlation. In contrast, the proposed EM-based data detector jointly processes readback signals from the upper and lower tracks as 2D data points, enabling multidimensional clustering of patterns such as {(-1, -1), (-1, +1), (+1, -1), (+1, +1)}. This allows the detector to exploit inter-track relationships and improve robustness against noise and TMR-induced distortions.

Furthermore, as TMR severity increases, the performance gap between the "Proposed system," the "System I," and the "System II" widens, indicating the effectiveness of the EM algorithm in both TMR prediction and data detection, making it a strong candidate for integration into next-generation SMR systems where TMR variability poses a significant challenge to reliable data retrieval.

## 5. Conclusion

This study investigates track misregistration (TMR) prediction and mitigation in shingled magnetic recording (SMR) systems using the Expectation-Maximization (EM) algorithm under an areal density (AD) of 2.0 Tb/in². The proposed EM-based TMR predictor consistently achieves over 70% accuracy, demonstrating robustness under severe TMR conditions and high electronic noise levels. Additionally, the EM-based data detector effectively mitigates TMR effects, delivering superior bit-error rate (BER) performance compared to both "System I" and "System II". These findings highlight the EM algorithm's strong potential for accurate TMR estimation and reliable data recovery, making it a promising solution for next-generation SMR systems facing increasing TMR variability.

## Acknowledgments

This work was financially supported by the School of Integrated Innovative Technology (SIITec), King Mongkut's Institute of Technology Ladkrabang (KMITL), Thailand, under Grant No. 2567-02-10-001.

## References

[1] R. Wood, Journal of Magnetism and Magnetic Materials **561**, 169670 (2022).
[2] Z. Jin, Ph.D. Dissertation, Experimental and theoretical studies of noise and off-track issues in magnetic recording systems. University of California, San Diego (2002).
[3] K. Kankhunthod and C. Warisarn, IEEE Access **11**, 41954 (2023).
[4] W. Busyatras, C. Warisarn, Lin M. M. Myint, and P. Kovintavewat, IEICT Trans. Electron **8**, 892 (2015).
[5] T. Yamaguchi and T. Atsumi, IFAC Proceedings Volumes **41**, 821 (2008).
[6] M. R. Elidrissi, K. S. Chan, and Z. Yuan, IEEE Trans. Magn. **50**, 1 (2014).
[7] L. M. M. Myint and P. Supnithi, IEEE Trans. Magn. **48**, 4590 (2012).
[8] S. Jeong and J. Lee, IEEE Trans. Magn. **59**, 1 (2023).
[9] H. Muraoka and S. J. Greaves, IEEE Trans. Magn. **51**, 1 (2015).
[10] Z.-M. Yuan, C. L. Ong, S. H. Leong, T. Zhou, and B. Liu, IEEE Trans. Magn. **46**, 1929 (2010).
[11] A. P. Dempster, N. M. Laird, and D. B. Rubin, Journal of the Royal Statistical Society. Series B (Methodological) **39**, 1 (1977).